Gene and Protein Expression Profiling of Human Ovarian Cancer Cells Treated with the Heat Shock Protein 90 Inhibitor 17-Allylamino-17-Demethoxygeldanamycin

Alison Maloney,[1] Paul A. Clarke,[1] Soren Naaby-Hansen,[3,4] Rob Stein,[3,5] Jens-Oliver Koopman,[3,4] Akunna Akpan,[3,4] Alice Yang,[3,4] Marketa Zvelebil,[3,4] Rainer Cramer,[3,4] Lindsay Stimson,[1] Wynne Aherne,[1] Udai Banerji,[1,2] Ian Judson,[1,2] Swee Sharp,[1] Marissa Powers,[1] Emmanuel deBilly,[1] Joanne Salmons,[1] Michael Walton,[1] Al Burlingame,[3,4] Michael Waterfield,[3,4] and Paul Workman[1]

[1]Haddow Laboratories, Cancer Research UK Centre for Cancer Therapeutics, The Institute of Cancer Research; [2]Royal Marsden NHS Foundation Trust, Sutton, Surrey, United Kingdom; [3]Ludwig Institute for Cancer Research and Departments of [4]Biochemistry and Molecular Biology and [5]Oncology, University College London, London, United Kingdom

Abstract

The promising antitumor activity of 17-allylamino-17-demethoxygeldanamycin (17AAG) results from inhibition of the molecular chaperone heat shock protein 90 (HSP90) and subsequent degradation of multiple oncogenic client proteins. Gene expression microarray and proteomic analysis were used to profile molecular changes in the A2780 human ovarian cancer cell line treated with 17AAG. Comparison of results with an inactive analogue and an alternative HSP90 inhibitor radicicol indicated that increased expression of HSP72, HSC70, HSP27, HSP47, and HSP90β at the mRNA level were on-target effects of 17AAG. HSP27 protein levels were increased in tumor biopsies following treatment of patients with 17AAG. A group of MYC-regulated mRNAs was decreased by 17AAG. Of particular interest and novelty were changes in expression of chromatin-associated proteins. Expression of the heterochromatin protein 1 was increased, and expression of the histone acetyltransferase 1 and the histone arginine methyltransferase PRMT5 was decreased by 17AAG. PRMT5 was shown to be a novel HSP90-binding partner and potential client protein. Cellular protein acetylation was reduced by 17AAG, which was shown to have an antagonistic interaction on cell proliferation with the histone deacetylase inhibitor trichostatin A. This mRNA and protein expression analysis has provided new insights into the complex molecular pharmacology of 17AAG and suggested new genes and proteins that may be involved in response to the drug or be potential biomarkers of drug action. [Cancer Res 2007;67(7):3239–53]

Introduction

Gene expression microarray and proteomic profiling facilitate screening for the response of thousands of mRNAs and proteins to anticancer agents and provide a means of obtaining a detailed molecular signature of drug action (1, 2). In addition, these methods may identify pharmacodynamic markers that can be used to evaluate drugs in clinical trials. Gene expression microarrays are increasingly used to investigate the molecular responses to cancer drugs in tumor cells (1). Although valuable, analysis of gene expression at the mRNA level alone cannot adequately predict protein expression or functional states. Therefore, proteomic approaches also have considerable potential in the drug development process (2).

Heat shock proteins (HSPs) are a major class of molecular chaperones that play a vital role in the cellular stress response and cancer (3, 4). One particular chaperone, HSP90, is of considerable current interest as a new cancer therapeutic target because of its essential role in maintaining the conformational stability and function of a number of oncogenic "client" proteins that are required for cellular proliferation, cell cycle regulation, apoptosis, invasion, angiogenesis, and metastasis (for review, see refs. 4, 5). The natural product HSP90 inhibitors radicicol, geldanamycin, and their derivatives exert their antitumor effect by inhibiting the intrinsic ATPase activity of HSP90, resulting in degradation of HSP90 client proteins via the ubiquitin-proteasome pathway (4, 5). Based on its novel mechanism of action and the potential for combinatorial effects on multiple oncogenic pathways and on all of the hallmarks of cancer (6), together with promising therapeutic effects in animal models (e.g., refs. 7–9), the geldanamycin analogue 17-allylamino-17-demethoxygeldanamycin (17AAG), a benzoquinone ansamycin, has completed phase I and is now in phase II clinical trials as the first-in-class HSP90 inhibitor (10, 11). Other HSP90 inhibitors are also in development (5).

Gene expression profiling studies have been done previously in a panel of human colon cancer cell lines following treatment with 17AAG (12). That study identified *HSC70* (*HSPA8*) and *HSP90β* (*HSPCB*) as 17AAG-responsive genes (12). Alongside depletion in levels of client proteins, such as c-RAF-1 and cyclin-dependent kinase 4 (CDK4), inducible HSP72 (*HSPA1A/HSPA1B*) has been used as a pharmacodynamic end point in phase I clinical trials of 17AAG (e.g., ref. 10). Indeed, this basic molecular signature has been used to show HSP90 inhibition in the tumor tissue of treated patients, and this was associated with prolonged stable disease in two patients with metastatic malignant melanoma (10). The cellular response to HSP90 inhibition has a complex nature that involves both multiple protein changes and effects on

Note: Supplementary data for this article are available at Cancer Research Online (http://cancerres.aacrjournals.org/).

P. Workman is a Cancer Research UK Life Fellow.

Conflict of interest: P. Workman's laboratory has received support from Vernalis, and HSP90 inhibitor technology from The Institute of Cancer Research/Vernalis collaboration has been licensed to Novartis.

Requests for reprints: Paul Workman, Haddow Laboratories, Cancer Research UK Centre for Cancer Therapeutics, 15 Cotswold Road, Belmont, Sutton, Surrey SM2 5NG, United Kingdom. Phone: 44-20-8722-4301; Fax: 44-20-8722-4324; E-mail: paul.workman@icr.ac.uk.

doi:10.1158/0008-5472.CAN-06-2968

transcription. We hypothesized that by using proteomic analysis in combination with gene expression microarray profiling we might identify additional molecular responses to 17AAG that would increase our understanding of the mechanism of action of the drug. This approach also has the potential to facilitate the discovery of new HSP90 client proteins as well as to suggest novel pharmacodynamic markers.

We now report a study in which the complementary approaches of mRNA and protein expression profiling have been used in parallel to examine expression changes in response to drug treatment in a human cancer cell line. Changes in mRNA and protein expression were determined following treatment of a human ovarian adenocarcinoma cell line with 17AAG. In addition, we sought to distinguish "on-target" effects (those which are a consequence of HSP90 inhibition) from "off-target" effects (those which relate to other interactions) by comparison of the molecular responses obtained following treatment with 17AAG with those seen with the chemically dissimilar HSP90 inhibitor radicicol or an inactive analogue of 17AAG. Selected known and novel expression changes were followed up by validation using Western blotting and investigation of functional and therapeutic significance.

Expression profiling studies revealed that around 3% of the total gene transcripts examined and 4% of the detectable proteins were responsive to 17AAG treatment. The changes seen involved a number of molecular chaperones, protein synthesis and degradation components, signaling molecules, and proteins involved in acetylation and methylation processes. Effects on HSP72, HSC70, HSP27 (HSPB1), HSP47, and HSP90β expression were identified as on-target effects of HSP90 inhibition. Together with HSP72, HSP27 was shown to exhibit increased expression in tumor biopsies from patients treated with 17AAG. Cellular protein acetylation was reduced following HSP90 inhibition, a possible consequence of altered expression changes of 17AAG-responsive acetylation proteins, including the histone acetyltransferase-1 (HAT-1). In addition, the protein arginine methyltransferase PRMT5 was identified as a new HSP90 binding partner and potential client protein, providing evidence that alterations in both protein acetylation and methylation may contribute to the mechanism of action of HSP90 inhibitors. This study shows that the combined deployment of the complementary techniques of proteomics and gene expression profiling is a useful strategy for examining molecular responses to novel cancer therapeutics, particularly those with complex effects, providing valuable information on the mechanism of drug action and enabling the identification of biomarkers of drug activity.

Materials and Methods

Cell culture and clinical biopsy specimens. Human cancer cell lines (A2780 ovarian, HCT116 colon, and WM266.4 melanoma) were obtained from the American Tissue Type Culture Collection (Rockville, MD). Cells were grown in DMEM containing 10% fetal bovine serum, 200 mmol/L glutamine, and 1× nonessential amino acids (Life Technologies, Paisley, United Kingdom) in a humidified atmosphere of 5% CO_2/95% air at 37°C. Biopsies were obtained pretreatment and posttreatment (24 h) with 17-AAG (450 mg/m^2) as part of the phase I clinical trial (10). Appropriate ethical committee approval and informed consent were obtained. Separate consent forms were signed before pretreatment and posttreatment biopsies.

Compounds. 17AAG (NSC330507) and the closely related, but essentially inactive, 4-aminobutyrate ester of 17AAG (NSC683201) were kindly supplied by Dr E. Sausville et al. (National Cancer Institute, Rockville and Bethesda, MD). Radicicol and trichostatin A (TSA) were obtained from Sigma Chemical Co. (Poole, United Kingdom). Compounds were stored as 2 mmol/L stocks in DMSO at −20°C and protected from light. All reagents were from Sigma unless stated otherwise and were of highest chemical grade.

Combination treatments. A2780 cells were seeded at 1,000 per well in 96-well plates. Sulfurhodamine blue staining was used to determine the IC_{50} at 96 h for TSA and 17AAG. These values were then used in combination studies according to the median effect analysis method of Chou and Talalay (13). Briefly, increasing concentrations of TSA and 17AAG were added at a ratio of 1:1 based on their respective IC_{50} values. Following a 96-h exposure, cells were stained with sulfurhodamine blue, and a combination index for nonexclusive interactions was calculated using an algorithm based on that described by Chou and Talalay (13). A combination index of 1 indicates an additive interaction; a combination index < 1 indicates a synergistic interaction; and a combination index > 1 indicates an antagonistic interaction.

Protein extraction. A2780 cells were plated in 75-cm^2 dishes at a density of 1×10^6 and left to attach for 24 h. Control cells were set up in quadruplicate, and 17AAG-treated cells set up in duplicate. Additional dishes were set up for cDNA microarray and Western blotting analysis. Cells were treated for 24 h with pharmacologically relevant, isoeffective concentrations of 17AAG (60 nmol/L) and radicicol (600 nmol/L), or, in some experiments, with an equimolar concentration of the inactive 17AAG analogue and radicicol in relation to 17AAG (60 nmol/L) in 10 mL medium.

Cell lysates for proteomic analysis were prepared in a laminar flow hood by scraping the cells into lysis buffer containing 8 mol/L urea (Merck, Poole, United Kingdom), 2 mol/L thiourea (Merck), 4% CHAPS, 65 mmol/L DTT (Merck), and a protease inhibitor cocktail (Roche, East Lewes, United Kingdom). Lysates were syringed using a 25-gauge needle and centrifuged at 14,000 × g for 5 min at 15°C. Protein concentrations, which were all in the range of 0.5 to 1 mg/mL, were determined using a Bradford assay.

For immunoblotting, cell pellets from A2780 cells in culture, or tissue from tumor biopsies from patients, were lysed in lysis buffer (150 mmol/L NaCl, 50 mmol/L Tris-HCl, 1% NP40, 0.2% SDS, 2 mmol/L phenylmethylsulfonyl fluoride, 10 μg/L aprotinin, 10 μg/L leupeptin, 1 mmol/L sodium orthovanadate, 0.5 mmol/L NaF, and 0.5 mmol/L β-glycerophosphate) for 20 min on ice and centrifuged at 14,000 × g, and the supernatant recovered. Protein concentration was determined using a bicinchoninic acid (BCA) protein assay (Pierce, Rockford, IL).

Two-dimensional gel electrophoresis and protein identification. Two-dimensional gel electrophoresis was done as described (14). Immobilized pH gradient strips, 18-cm pH3-10NL (Amersham Pharmacia Biotech, Little Chalfont, United Kingdom), were used for the first dimension separation of 150 μg protein lysate followed by second dimension separation on 20-cm gradient PAGE gels (Oxford Glycosciences, Oxford, United Kingdom). Following fixation and post-staining with silver stain, gels were scanned, and the resulting images were analyzed using Melanie II software and in-house analysis tools (15). All gels were run in duplicate. The mean value of % volume for features matched between duplicate gels was used for quantitative analysis. To quantitate temporal changes in matched features where the feature of interest could not be detected in one of the gels, the spot outline was copied to the relevant gel image from a matching gel, and the missing spot was assigned a value equivalent to the background volume within the spot outline. Spots showing systematic variation in intensity as a result of 17AAG treatment were excised from the gel using a robotic cutter.

Protein identification was done by matrix-assisted laser desorption/ionization mass spectrometry (MALDI MS) as follows. The excised gel spots were subjected to reduction and alkylation using DTT (Pierce) and iodoacetic acid (Sigma, Poole, United Kingdom) followed by in-gel digestion with modified trypsin (Promega, Southampton, United Kingdom) similar to methods previously described (16, 17).

MALDI MS was done on a Reflex III (Bruker Daltonik, Bremen, Germany) mass spectrometer in the reflector mode using delayed extraction. A 0.5-μL aliquot of the in-gel digest was mixed with 1 μL of

a saturated aqueous 2,5-dihydroxybenzoic acid solution directly on the target plate and subsequently dried under a warm stream of air. The peptide mass fingerprint recorded was internally calibrated using the tryptic autolysis product ions at the monoisotopic masses of m/z 842.5100 and 2,211.1046. The MS-Fit program (ProteinProspector, University of California at San Francisco, San Francisco, CA) was used for peptide mass mapping and searching the National Center for Biotechnology Information (NCBI) protein database, similar to earlier descriptions (18). The peptide mass tolerance was set to ±100 ppm.

cDNA microarrays. Cells were lysed in denaturing buffer [2.7 mol/L guanidium thiocyanate, 1.3 mol/L ammonium thiocyanate, 100 mmol/L sodium acetate (NaOAc; pH 4)] and extracted twice with saturated phenol [0.61 g/mL phenol, 16% v/v glycerol, 100 mmol/L NaOAc (pH 4)] and chloroform. Polyadenylated mRNA [poly(A^+) mRNA] was prepared from total RNA using oligo (dT) cellulose (Micro-FastTrack 2.0, Invitrogen, Paisley, United Kingdom). Poly(A^+) mRNA was concentrated using Centricon spin columns (Millipore Ltd, Watford, United Kingdom) to a final volume of 5 μL.

cDNA microarrays were done according to the procedure outlined in (12). All array experiments were replicated independently: 17AAG (n = 4) and radicicol and NSC683201 (n = 2). Lowstra analysis fits a Lowess curve to remove any systematic bias from the experiment. Outliers from the straightened data set are detected using a Student's t test, such that points furthest from the straight line are statistically significant (98% confidence level) from the points lying along the straight line (19). Cluster and Treeview algorithms[6] were used to obtain self-organizing maps of the gene expression data sets (20).

SDS-PAGE and immunoblotting. Samples (typically 75 μg protein) were denatured in Laemmli loading buffer [10% glycerol, 5% β-mercaptoethanol, 2% SDS, 62.5 mmol/L Tris (pH 6.8), 0.05% bromophenol blue] and were separated on 4% to 20% Tris-Glycine polyacrylamide gels (Invitrogen) using the Novex X-Cell Surelock Mini electrophoresis system (Invitrogen). Proteins were electrotransferred to a 0.22-μm nitrocellulose membrane (Invitrogen), and membranes were blocked for at least 1 h in casein blocking buffer [150 mmol/L NaCl, 10 mmol/L Tris base, 0.25 mmol/L thimerosal, 0.5% Hammarsten grade casein (pH 7.6)]. Membranes were exposed to primary antibody in casein blocking buffer overnight. The following antibodies were used: anti-rabbit polyclonal c-RAF-1 antibody (C-12; Santa Cruz, CA); 1.0 μg/mL mouse monoclonal HSP72 (SPA-840; Stressgen Biotechnologies, Victoria, Canada), 0.9 μg/mL mouse monoclonal HSP27 antibody (SPA-800; Stressgen), 1.0 μg/mL anti-mouse monoclonal HSP72/HSC70 antibody (SPA-820; Stressgen), 1.3 μg/mL rat monoclonal HSP90α antibody (Stressgen); 1:1,000 dilution rabbit polyclonal PRMT5 methyltransferase antibody (Cell Signaling Technology, Boston, MA); 1:1,000 rabbit polyclonal c-AKT antibody (Cell Signaling Technology); 1:1,000 rabbit polyclonal ERBB2 (C-18; Santa Cruz); 1:1,000 rabbit polyclonal CDK4 (C-22; Santa Cruz). Membranes were washed twice with PBS containing 0.05% Tween 20. Visualization of the bound primary antibody was done by probing with anti-mouse IgG horseradish peroxidase (HRP) or anti-rabbit IgG HRP at 1:1,000 dilution (Amersham Pharmacia Biotech), and the membranes washed four times. Immunodetection was carried out using enhanced chemiluminescence reagent (Pierce) and exposure to photographic film (Amersham Pharmacia Biotech).

Acetylation ELISA. A2780 cells (8×10^2) were seeded into 96-well plates and left to attach for 36 h. The cells were then treated with a concentration range of 17AAG, radicicol, NSC683201, or the histone deacetylase inhibitor TSA for 24 h. Cells were then fixed (3% formaldehyde, 0.25% glutaraldehyde, 0.25% Triton X-100) and blocked for 1 h in 5% milk in PBS at 37°C. Cells were washed in 0.1% Tween 20/H_2O and incubated with an antibody to acetylated histone/protein (ab-193, Abcam Ltd., Cambridge, United Kingdom) in PBS (1:2,000 dilution) for 1 h at 37°C. Cells were washed again in 0.1% Tween 20/H_2O and incubated with europium-labeled rabbit IgG in DELFIA assay buffer (Perkin-Elmer Life And Analytical Sciences, Inc., Boston, MA; 0.2 μg/mL) for 1 h at 37°C. Finally, enhancement solution (Perkin Elmer Life Sciences, MA) was added to the cells, and the DELFIA absorbance was measured using a spectrophotometric plate reader. Protein measurements were then carried out on the same plate using the BCA protein assay (Pierce). Results were corrected for protein concentration by dividing the DELFIA absorbance by the protein absorbance, and results were expressed as % control cells.

Results

Gene expression profiling following treatment with 17AAG, an inactive analogue, and radicicol. 17AAG inhibits the growth of A2780 human ovarian tumor cells with an IC_{50} for a 96-h treatment of 12 nmol/L (7). A2780 cells were treated for 24 h with 60 nmol/L 17AAG (this equates to 5× IC_{50} or IC_{90} for the 96-h exposure) or with an isoeffective concentration (600 nmol/L) of the chemically dissimilar HSP90 inhibitor radicicol. To identify off-target effects, cells were also treated with 60 nmol/L of the essentially inactive 4-aminobutyrate ester of 17AAG (NSC683201), which has no effect on HSP90 ATPase activity or cancer cell proliferation up to a concentration of 40 μmol/L (data not shown). In selecting an equimolar concentration of NSC683201 and 17AAG, we considered that effects of the chemical backbone (off-target) would be the same when tested at the same equimolar concentration, whereas HSP90 (on-target) effects would be restricted to 17-AAG. Hence, both compounds were used at 60 nmol/L. Control cells were treated with vehicle (0.1% DMSO) for 24 h. cDNA microarrays of 4,132 cDNA clones corresponding to genes of known identity were used to analyze gene expression changes. The complete list of expression changes in response to 17AAG, radicicol, and NSC683201 in A2780 cells is provided as Supplementary Data.

With all three compounds, the expression of the majority of genes remained unchanged. Using Lowstra analysis (19), the expression levels of 129, 47, and 12 genes (3%, 1%, and 0.3%) were shown to be significantly (P < 0.02) increased or decreased at the mRNA level with 17AAG, radicicol, and NSC683201, respectively (Fig. 1*A*). The majority of these gene expression changes were observed in response to only one of the compounds. However, expression of 13 of 145 HSP90 inhibitor–responsive genes were altered in response to both 17AAG and the chemically dissimilar HSP90 inhibitor radicicol and could thus be classified as likely on-target effects (Fig. 1*A*). Such on-target changes may be a direct result of HSP90 inhibition or alternatively may be a consequence of the downstream effects of HSP90 client protein depletion. We reasoned that changes in mRNA expression that were seen with both the active and inactive benzoquinone ansamycins, or with just one of the three compounds examined, are less likely to be a consequence of HSP90 inhibition and are more probable off-target effects. Of interest, only one gene showed altered expression in response to both of the benzoquinone ansamycins 17AAG and NSC683201, although they share the same chemical backbone. In addition, only one gene showed altered expression with both radicicol and NSC683201, and a single gene exhibited decreased expression with all three compound treatments.

Genes classified as significantly altered in expression at the mRNA level following treatment with 17AAG are catalogued in Table 1. Genes showing significant expression changes are grouped according to their function, and genes for which the mRNAs that exhibited a >2-fold increase are indicated in bold italics. Genes corresponding to a number of HSPs were shown to exhibit increased expression in response to both of the active HSP90 inhibitors but not NSC683201. These genes included *HSC70,*

[6] http://rana.stanford.edu

A

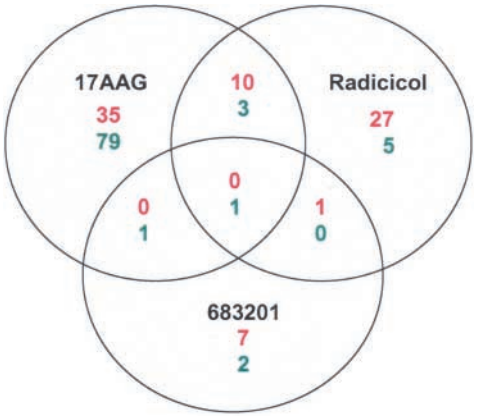

Figure 1. *A,* Venn diagram illustrating the number of genes that show altered expression at the mRNA level in response to 17AAG, radicicol, and the essentially inactive 17AAG analogue NSC683201 using Lowstra statistical analysis. *Red numbers,* genes that show increased expression following treatment; *green numbers,* genes that show decreased expression in response to these agents. Numbers in the circle intersections relate to genes that exhibit altered expression in common with agents named in the corresponding circles. *B,* hierarchical clustering using self-organizing maps of mRNA expression changes in A2780 cells treated with 17AAG, radicicol, and NSC683201. Gene expression data were analyzed using the clustering algorithm of Eisen et al. (36). *Green signal,* gene for which expression is decreased; *red signal,* gene for which expression is increased; *black*, no difference. The intensity of the color is proportional to the degree of difference from the median. The dendrogram illustrates all mRNAs identified as outliers using the Lowstra statistical program ($P < 0.02$) following treatment with 17AAG, radicicol, and the essentially inactive 17AAG analogue NSC683201. *Yellow boxes,* selected clusters. *Cluster #1,* group of genes that are up-regulated following treatment with both active HSP90 inhibitors and includes a number of HSP and HSP cochaperone genes. *Cluster #2,* group of genes that are down-regulated following treatment with both active HSP90 inhibitors and includes genes that have been shown to be regulated by MYC.

B

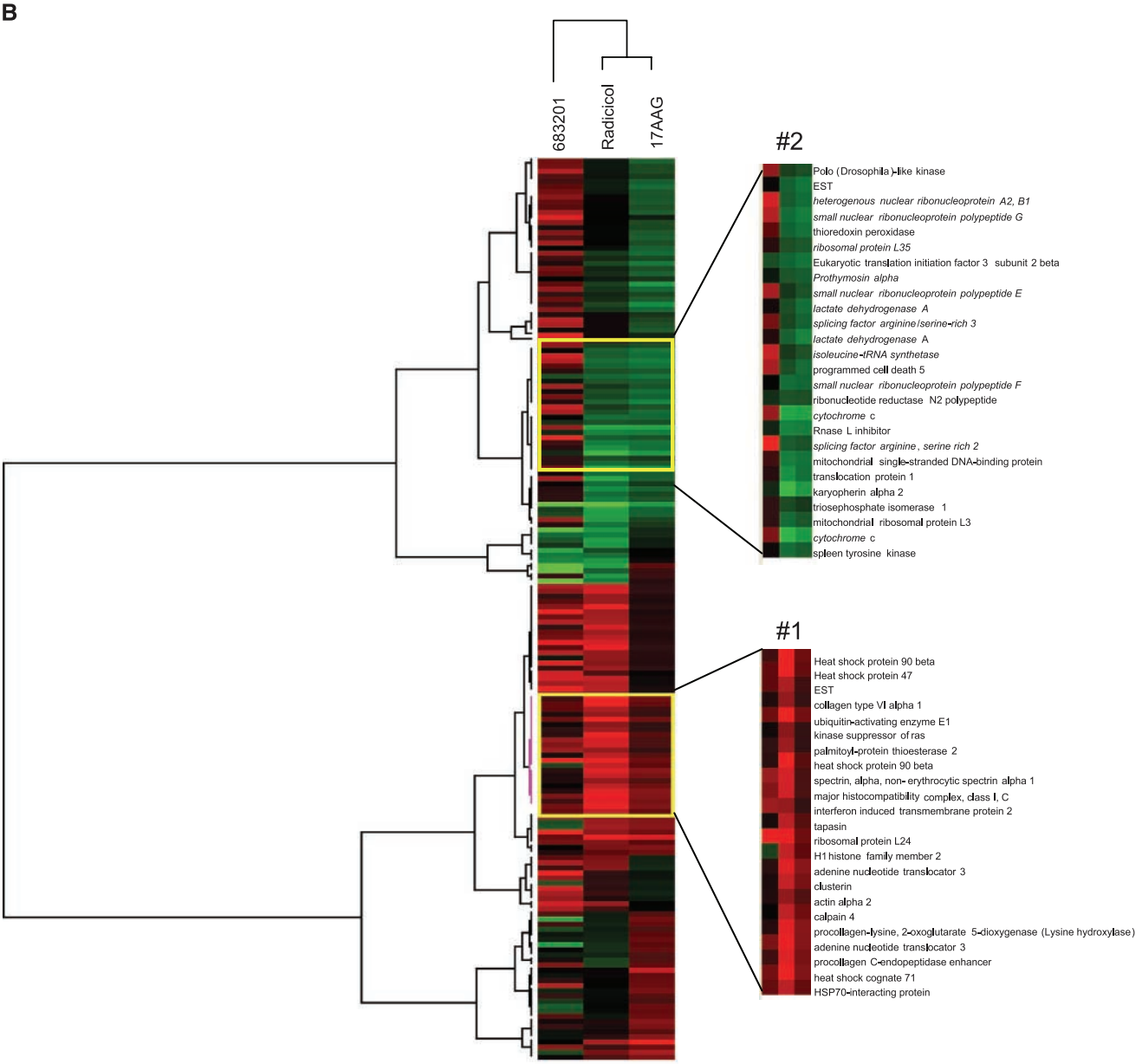

HSP90β, and *HSP47*. Other genes exhibiting increased expression in response to HSP90 inhibitors were involved in protein synthesis and degradation, cell cycle, signal transduction, and RNA processing and transcription (Table 1). Genes with decreased expression at the mRNA level following HSP90 inhibition were also grouped by function. These functions include protein folding, protein synthesis and degradation, signal transduction, cell cycle, RNA processing, transcription, chromatin, transport, metabolism, apoptosis, cytoskeleton, and detoxification (Table 1).

By grouping genes showing significantly altered expression using a self-organizing map, A2780 cells treated with isoeffective concentrations of 17AAG and radicicol were shown to exhibit a much more similar overall gene expression signature than that obtained following treatment with the inactive 17AAG analogue NSC683201 (Fig. 1*B*). On-target effects of HSP90 inhibition that were identified using Lowstra analysis and listed in Table 1 were also shown to be clustered together.

One cluster of genes with increased expression following HSP90 inhibition (Fig. 1*B, #1*) contained genes involved in the HSP90 chaperone complex, including the previously mentioned *HSP90β, HSC70*, and *HSP47* (Fig. 1*B*; Table 1). All of these genes were induced in response to the two active HSP90 inhibitors, but less so with the essentially inactive NSC683201 (Fig. 1*B*; Table 1). Because HSP47 is known to stabilize and correctly fold procollagen, it is particularly interesting that the expression of both *procollagen c-endopeptidase enhancer* (*PCOLCE*) and *procollagen-lysine, 2-oxyglutarate* (*PLOD*) genes are also increased within this cluster.

Another interesting cluster (Fig. 1*B, #2*) contains the genes with decreased expression in response to both of the active HSP90 inhibitors but increased expression with NSC683201 (Fig. 1*B*). This corresponds to a gene cluster shown to be decreased in expression in tumors from rectal cancer patients treated with 5-fluorouracil (5-FU; ref. 21). These genes have been shown by other groups to be regulated by MYC (22) and are marked with an asterisk in Table 1.

Two-dimensional proteomic analysis following 17AAG treatment. Cell lysates were analyzed using two-dimensional gel electrophoresis to detect changes in the A2780 proteome following 17AAG treatment. Figure 2*A* shows a typical two-dimensional gel of A2780 control cell lysates. Using a 1.5-fold cutoff, the analysis identified 42 altered protein spots, which accounted for ~3% of the total number of detectable proteins. From these 42 spots, 26 proteins could be annotated from the NCBI database. Table 2 lists the names of identified proteins, their NCBI database accession numbers, spot designation, experimental and reported isoelectric point and molecular weight values, along with sequence coverage. The functions of 17AAG-responsive proteins are listed in Table 3 with appropriate references.

A time-dependent induction of members of the molecular chaperone machinery, including HSP72, HSC70, and HSP27, was observed following 17AAG treatment (Table 2; Fig. 2*B*). In addition, the mitochondrial HSP70 isoform mortalin-2 (GRP75/HSPA9B) was also shown to be induced by 17AAG. HSP72 (spot nos. 366 and 326) and HSP90β (spot nos. 138 and 142) were detectable in two protein spots, most likely as a consequence of posttranslational modifications or alternative mRNA splicing. In addition, a protein spot corresponding to the sequence encoded by *C14ORF3* was induced in a similar manner to HSP70 following 17AAG treatment. Further studies published previously revealed that this protein was in fact a novel cochaperone AHA1, which has an important role in the activation of HSP90 ATPase activity (23). The targets of 17AAG, HSP90α (HSPCA), and HSP90β protein levels were shown to increase at 8 h and decrease at 24 h (Table 2). Expression of HnRNP3 (hnRNP 2H9A), a member of the heterogeneous nuclear ribonucleoprotein family, was found to be decreased in response to 17AAG. This protein has been shown to be involved in early heat shock–induced splicing arrest (24).

Another group of proteins showing altered expression following 17AAG treatment were those involved in the posttranslational modifications of proteins, including histones. A decrease in the expression of both HAT-1 and the protein methyltransferase PRMT5 (SKB1/JBP1) was observed in response to 17AAG (Table 2; Fig. 2*B*). In addition, the levels of heterochromatin protein 1 (HP1) were increased by 17AAG.

Confirmation of HSP expression changes by Western blotting. As a follow-up to the gene expression microarray and two-dimensional proteomic gel analysis, a number of HSP changes observed were analyzed in more detail using Western blotting. This analysis was carried out on the same samples that were used in the gene expression and proteomic screening so that the results were directly comparable. c-RAF-1 was also studied because this and other low-abundance client proteins were not detectable in the proteomic profiling. Protein expression changes were examined over a 72-h time course following treatment with 60 nmol/L 17AAG. As expected, depletion of the client protein c-RAF-1 by 17AAG was consistent with HSP90 being inhibited in the samples used for gene expression and proteomic analysis (Supplementary Fig. S1*A* and *B*). HSP72 and HSP27 were induced in a time-dependent manner by growth-inhibitory concentrations of 17AAG and remained above control levels throughout the entire time course (Supplementary Fig. S1*A*).

Although HSF-1–dependent transcription of HSPs has been observed previously in response to HSP90 inhibitors (23), it has not been entirely clear whether this is truly an on-target effect of HSP90 inhibition or a general stress response. To confirm whether these responses were on-target effects of HSP90 inhibition, HSP expression changes were assessed in A2780 cells treated with isoeffective ($5\times$ IC_{50}) concentrations of 17AAG or radicicol for 24 h. In addition, these responses were also compared with those to equimolar concentrations of 17AAG, radicicol, and NSC683201. HSP72, HSC70, and HSP27 were confirmed as likely on-target effects of HSP90 inhibition as their protein levels were induced by growth-inhibitory concentrations of 17AAG and radicicol but markedly less so by the much less active 17AAG analogue and with the lower concentration of radicicol (Supplementary Fig. S1*B*). Interestingly, HSP90α protein expression was increased with all three compounds, including the essentially inactive 17AAG analogue, suggesting that increased HSP90α expression may not solely be an on-target effect.

Detection of HSP27 induction in tumor biopsies from patients treated with 17AAG. Protein expression changes in response to drugs are increasingly used as potential pharmacodynamic end points in clinical studies and are essential for investigating new molecular targeted cancer therapies (25), including HSP90 inhibitors (see ref. 6). Limited tumor biopsy samples were available from patients treated with 17AAG. Supplementary Figure S1*C* shows typical Western blots of tumor tissue taken from two patients: one with melanoma and the other with mesothelioma (ascitic fluid) before and after treatment with 450 mg/m^2 17AAG as part of a phase I clinical trial (10). As expected, both HSP72 induction and c-RAF-1 depletion were found to occur in tumor tissue and cells following 17AAG treatment in these two patients. In addition, the expression of HSP27 was also shown to increase in

Table 1. Genes that show altered expression at the mRNA level in A2780 human ovarian cancer cells treated with 17AAG

Decreased

Accession no.	Gene name
Signal transduction	
AA235332	*Ras suppressor protein 1* (*RSU1*)
AA424700	*MAD homologue 5* (*SMAD5*)
AA455067	*Synuclein α* (*SNCA*)
AA479741	*TNFRSF1A modulator* (*BRE*)
AA490011	*Latent transforming growth factor-β binding protein 1* (*LTBP1*)
R44288	***calmodulin 2 (CALM2)****
R59598	*spleen tyrosine kinase* (*SYK*)
HSP	
AA669341	*p23 cochaperone* (*P23*)
H07880	*Chaperonin containing TCP1 subunit 6A* (*CCT6A*)
RNA processing/splicing	
AA126911	*Heterogeneous nuclear ribonucleoprotein A1* (*HNRPA1*)*
AA133577	*Small nuclear ribonucleoprotein polypeptide G* (*SNRPG*)*
AA454585	*Splicing factor arginine, serine-rich 2* (*SFRS2*)*
AA487442	*Heterogeneous nuclear ribonucleoprotein G* (*HNRPG*)*
AA504272	*Heterogeneous nuclear ribonucleoprotein M* (*HNRPM*)*
AA598400	*Splicing factor arginine/serine-rich 3* (*SFRS3*)
AA668189	*Small nuclear ribonucleoprotein polypeptide F* (*SNRPF*)*
AA599116	*Small nuclear ribonucleoprotein polypeptides B, B1* (*SNRPB*)*
AA678021	*Small nuclear ribonucleoprotein polypeptide E* (*SNRPE*)*
H05899	*Heterogeneous nuclear ribonucleoprotein C1, C2* (*HNRPC*)*
H54020	*Splicing factor arginine/serine-rich 7* (*SFRS7*)^{RAD}
W02101	*Heterogeneous nuclear ribonucleoprotein A2, B1* (*HNRPA2B1*)*
W72693	*Heterogeneous nuclear ribonucleoprotein A, B* (*HNRPAB*)*
Protein synthesis	
AA410636	*Isoleucine-tRNA synthetase* (*IARS*)*
AA450205	*Translocation protein 1* (*TLOC1*)^{RAD}
AA599178	*Ribosomal protein L27a* (*RPL27A*)*
AA625634	*Ribosomal protein L35* (*RPL35*)*
AA633768	*Ribosomal protein L24* (*RPL24*)*
AA664241	*Nascent-polypeptide-associated complex α* (*NACA*)
AA668301	*Ribosomal protein S16* (*RPS16*)*
AA669359	*Ribosomal protein L36a* (*RPL36A*)
AA683050	*Ribosomal protein S8* (*RPS8*)*
AA775364	*Ribosomal protein L30* (*RPL30*)*
H09590	*Eukaryotic translation initiation factor 4A isoform 1* (*EIF4A1*)*
H29485	*La autoantigen* (*SSB*)
T70056	*RNase L inhibitor* (*ABCE1*)
Apoptosis	
AA156940	*Programmed cell death 5* (PDCD5)
R52654	***Cytochrome c (HCS)***^{RAD}*
R53311	***cytochrome c (HCS)****

Table 1. Genes that show altered expression at the mRNA level in A2780 human ovarian cancer cells treated with 17AAG (Cont'd)

Decreased

Accession no.	Gene name
Protein degradation	
AA430504	*Ubiquitin carrier protein E2-C* (*UBCH10*)
AA598815	*Proteasome subunit α type 5* (*PSMA5*)
AA863149	*Proteasome α type 7 subunit* (*PSMA7*)*
Cell cycle	
AA481076	*MAD2-like 1* (*MAD2L1*)
AA488332	*Proliferation-associated 2G4* (*PA2G4*)
N21624	*14-3-3 ε* (*YWHAE*)
AA629262	*Polo (Drosophia)-like kinase*
Chromatin	
AA625662	*HAT-1*
AA868008	*H4 histone family member G* (*H4FG*)^{RAD,INACTIVE}
N64051	*Werner syndrome* (*WRN*)
Transcription	
AA099534	*Activated RNA polymerase II transcription cofactor 4* (*PC4*)
AA630017	*Transcription elongation factor B polypeptide 2* (*TCEB2*)
AA773894	*Zinc finger protein 43* (*HTF6*)
AA873691	*RNA polymerase II polypeptide L* (*POLR2L*)*
AA894687	*Subunit of NFAT* (*NF45*)
T55801	*General transcription factor IIA 2* (*GTF2A2*)
Metabolism	
AA171613	*Carbonic anhydrase XII* (*CA12*)
R15814	*Malate dehydrogenase 1* (*MDH1*)
AA431433	*ATP synthase H+ transporting, mitochondrial F0 complex subunit e* (*ATP5I*)
AA453471	*GM2 ganglioside activator protein* (*GM2A*)
AA460728	*Voltage-dependent anion channel 3* (*VDAC3*)
AA487206	*Glyceronephosphate O-acyltransferase* (*GNPAT*)
AA644234	*ATP synthase H+ transporting, mitochondrial F1 complex, γ 1* (*ATP5C1*)
H05914	*Lactate dehydrogenase A* (*LDHA*)*
H05914	*Lactate dehydrogenase A* (*LDHA*)*
R15814	*Malate dehydrogenase 1* (*MDH1*)
AA663983	*Triosephosphate isomerase 1* (*TPI1*)
Structure	
AA113872	*Clathrin light polypeptide* (*CLTA*)
H67086	*Similar to Saccharomyces cerevisiae SSM4* (*TEB4*)
N20335	*Clathrin, light polypeptide* (*CLTB*)
AA434144	*Claudin 3* (*CLDN3*)
AA634103	*Thymosin β 4* (*TMSB4X*)
AA644679	*Cytoplasmic dynein light polypeptide* (*PIN*)
Transport	
AA234671	*ATP-binding cassette sub-family D member 3* (*ABCD3*)
AA487623	*Gap junction protein α 1* (*GJA1*)
T71316	*ADP-ribosylation factor 4* (*ARF4*)
AA676460	*Karyopherin α 2* (*KPNA2*)^{r}
Proliferation	
AA442991	*Prothymosin α* (*LOC51115*)*
DNA synthesis/repair	
AA775355	*DNA repair protein* (*XRCC5*)

(*Continued on the following page*)

Table 1. Genes that show altered expression at the mRNA level in A2780 human ovarian cancer cells treated with 17AAG (Cont'd)

Decreased

Accession no.	Gene name
AA465203	*Mitochondrial single-stranded DNA-binding protein* (*SSBP*)
Detoxification	
AA459663	*Thioredoxin peroxidase* (*AOE372*)
H19203	*Peroxiredoxin 3* (*PRDX3*)*
Unknown	
AA460286	*Guanine nucleotide binding protein 10* (*GNG*)
AA187351	*Ribonucleotide reductase M2 polypeptide*
H49443	*EST*^{INACTIVE}
T68317	*EST*

Increased

Accession no.	Gene name
Signal transduction	
H88143	*Kinase suppressor of ras* (*KSR*)
N36174	*5-Hydroxytryptamine receptor 2B* (*HTR2B*)
R40460	*Phosphatidylinositol 4-kinase catalytic α* (*PIK4CA*)
R96626	*Small inducible cytokine subfamily A member 14* (*SCYA14*)
AA490300	*PDGFA associated protein 1*
AA862371	*IFN-induced transmembrane protein 2* (*IFITM2*)
H79047	*Insulin-like growth factor binding protein 2* (*36 kDa*)
AA644448	*Protein tyrosine phosphatase, receptor type, U*
T72202	*Signal transducer and activator of transcription 6, interleukin-4 induced*
N90246	*EphA1*
HSP	
AA629567	*Heat shock cognate 71* (*HSPA8*)^{RAD}*
H65676	*Hsp70-interacting protein* (*HIP*)
R44334	*Hsp90 β* (*HSPCB*)^{RAD}*
R71093	*Hsp47* (*SERPINH2*)^{RAD}
Protein synthesis	
R43766	***Eukaryotic translation elongation factor 2 (EEF2)***^{RAD}*
Protein degradation	
AA430512	*Serine (or cysteine) proteinase inhibitor clade B member 9* (*SERPINB9*)
AA670200	*Procollagen C-endopeptidase enhancer* (*PCOLCE*)^{RAD}
H15456	*Calpain 1* (*CAPN1*)
R61332	*Ubiquitin-activating enzyme E1* (*UBE1*) ^{RAD}
AA427725	***Carboxypeptidase X (CPZ)***
Transcription	
AA235706	*RNA polymerase II TBP-associated factor H* (*TAF2H*)
AA428551	*Sex determining region Y-box 22* (*SOX22*)
AA436409	*TAR RNA-binding protein 2* (*TARBP2*)
AA454218	*TATA box binding protein–associated factor RNA polymerase I C* (*TAF1C*)
AA633811	*Nuclear factor interleukin 3 regulated* (*NFIL3*)
Chromatin	
H24688	*SWI, SNF-related matrix-associated actin-dependent regulator of chromatin subfamily c member 2*
Transport	
AA069770	*Potassium voltage–gated channel Shab-related subfamily member 1* (*KCNB1*)

Table 1. Genes that show altered expression at the mRNA level in A2780 human ovarian cancer cells treated with 17AAG (Cont'd)

Increased

Accession no.	Gene name
AA402874	*Phospholipid transfer protein* (*PLTP*)
AA452148	*Syntaxin 5A* (*STX5A*)
AA490044	*Inositol transporter* (*SLC5A3*)
H61243	*Uncoupling protein 2* (*UCP2*)
Metabolism	
AA455126	*ATP synthase H+ transporting mitochondrial F0 complex subunit c isoform 2* (*ATP5G2*)
AA663439	*Adenine nucleotide translocator 3* (*ANT3*)^{RAD}
R61295	*Adenine nucleotide translocator 3* (*ANT3*)
Structure	
AA400329	*Neurofilament 3* (*NEF3*)
AA877166	***Myosin regulatory light chain 2 (MYLR2)***^{RAD}
H73276	*Actin related protein 2, 3 complex subunit 3* (*ARPC3*)
T60117	*Spectrin, α, non-erythrocytic spectrin α 1* (*SPTAN1*)^{RAD}
Cell cycle	
N58511	*Cyclin I* (*CCNI*)^{RAD}
RNA processing	
AA443039	*Dual specificity phosphatase 11* (*RNA, RNP complex 1-interacting*)
Unknown	
AA045508	***Adenylyl cyclase-associated protein 2***
AA487231	*Cathepsin H*
N29376	*Myeloid cell nuclear differentiation antigen*
R51835	*EST*
R79935	*EST*

NOTE: Cells were treated with a pharmacologically active concentration of 60 nmol/L 17AAG. mRNA expression was determined by cDNA microarray profiling. All array experiments were replicated independently: 17AAG (n = 4), radicicol (n = 2), and NSC683201 (n = 2). The Lowstra algorithm was used to identify genes that were outliers (P < 0.02). Genes for which expression was also altered by radicicol (600 nmol/L) or NSC683201 (60 nmol/L) are indicated by RAD or INACTIVE, respectively. Genes in bold italics were altered >2-fold compared with control.
*Indicates those genes that have been shown to be regulated by MYC (see text).

these two patients following treatment with 17AAG and could potentially be used as an additional pharmacodynamic marker in the clinical evaluation of HSP90 inhibitors. Because HSP72, HSC70, and HSP27 have antiapoptotic roles (3, 26), their increased expression could be of therapeutic significance.

Effects of HSP90 inhibition on cellular protein acetylation. As mentioned above, a number of proteins and genes involved in cellular protein acetylation processes exhibited altered expression after treatment of A2780 cells with 17AAG. The HAT-1 protein showed reduced expression in response to 17AAG (Fig. 2*B*), with a concomitant decrease observed at the mRNA level using cDNA microarray analysis (Table 1). We hypothesized that changes in the expression of chromatin-modifying enzymes could affect acetylation of cellular proteins. An ELISA was used to examine

total protein acetylation in A2780 cells following exposure to 17AAG, radicicol, and the inactive 17AAG analogue NSC683201. Interestingly, acetylation was inhibited 23% by both 17AAG and radicicol ($P < 0.05$), whereas the inactive analogue had very little effect on acetylation (Fig. 3*A*). As expected, the histone deacetylase inhibitor TSA was shown to increase acetylation by 30% above control levels ($P < 0.05$; Fig. 3*A*). Of note, when 17AAG was added together with TSA to the cells, a significant decrease in acetylation was observed compared with both the untreated control and TSA alone–treated cells ($P < 0.05$; Fig. 3*A*). Combination studies of TSA with 17AAG gave a combination index of 2.92 ± 0.64 (SD, $n = 3$). This indicated an antagonistic interaction that was consistent with the data from the acetylation assay described above (Fig. 3*B*). These results show that

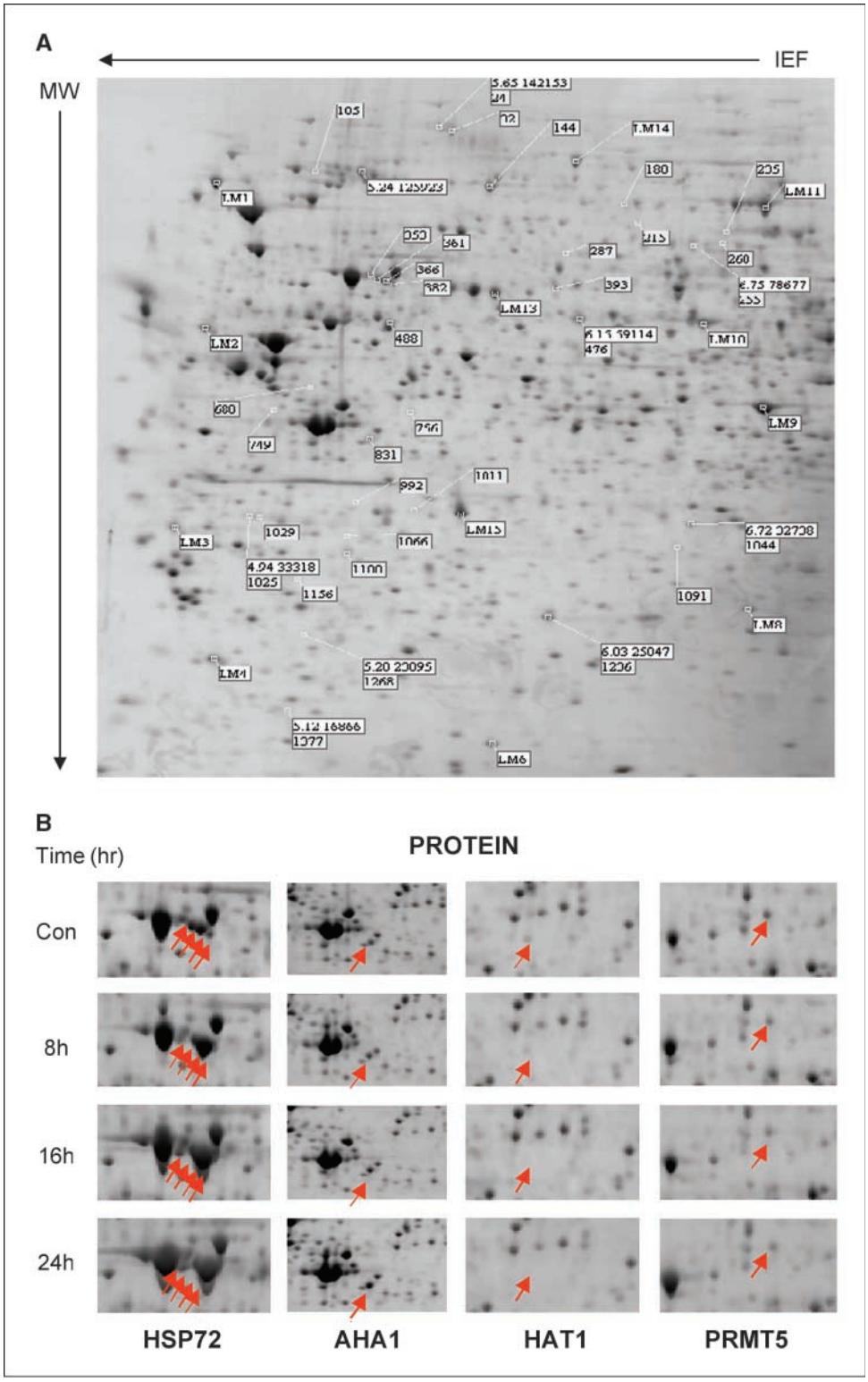

Figure 2. *A,* representative two-dimensional gel from A2780 human ovarian cancer cell control protein lysates. Proteins from cell lysates were separated according to both their molecular weight and their isoelectric point using two-dimensional electrophoresis. *LM,* landmark proteins that were used to align spots on gels. Annotated proteins responsive to 17AAG are indicated by gel spot number and are listed in Table 3. All gels were carried out in duplicate for each sample. *B,* selected regions of two-dimensional gels illustrating individual protein expression changes following 17AAG treatment. Protein expression of HSP72 AHA1, HAT-1, and PRMT5 across a 24-h time course following treatment with 17AAG.

Table 2. Annotated proteins that showed altered expression in A2780 human ovarian cancer cells following treatment with 17AAG

Protein spot no.	Gel spot mass*	Gel spot pI*	Protein name	Protein mass †	Protein pI †	Peptide match ‡	NCBI accession no.	Expression ratios		
								8 h	16 h	24 h
32	140,149	5.69	Leucine-rich protein (LRPPRC)	145,202	5.50	14, 16%	1730078	0.9	0.5	0.4
129	93,779	6.73	HSP90α (HSPCB/HSPCA/HSP90A)	84,660	4.94	23, 32%	72219	0.6	2.4	0.4
138	92,610	6.63	HSP90β (HSPCB/HSPC2/HSP90B)	84,844	5.26	32, 39%	11277141	1.3	2.7	0.4
142	92,031	6.45	HSP90β (HSPCB/HSPC2/HSP90B)	83,265	4.97	21, 30%	11419019	0.8	3.65	0.5
144	114,885	5.81	Glucosidase II α subunit (G2AN)	106,901	5.71	32, 36%	7661898	0.8	0.3	0.4
180	108,158	6.38	Mini chromosome maintenance protein 4 (MCM4)	103,047	8.39	14, 21%	940536	0.8	0.4	0.4
223	76,156	5.45	HSP70 9B (mortalin-2)	73,728	6.03	8, 14%	12653415	1.2	1.1	1.5
255	78,677	6.75	Glutamine:fructose-6-phosphate amidotransferase-1 (EFAT)	76,748	6.39	22, 30%	4503981	0.6	0.6	0.5
326	66,372	5.27	Hsc70-8 (HSPA8)	73,951	5.38	21, 32%	11436031	1.4	1.3	1.6
			HSP72 (HSP701B)	70,026	5.48	13, 26%	4885431			
353	69,838	5.44	HSC70 (HSPA8)	73,951	5.38	21, 38%	11436031	0.9	1.8	2.3
361	68,361	5.46	Annexin (ANXA6)	75,860	5.41	34, 59%	35218	1.0	0.8	0.9
			HSP70 (HSPA8)	73,951	5.38	11, 19%	11436031			
366	67,780	5.49	HSP72 (HSP701B)	70,026	5.48	11, 23%	4885431	6.4	10.1	10.7
382	66,916	5.51	Annexin A6 (ANXA6)	75,860	5.41	29, 41%	35218	1.1	1.6	1.6
			HSP72 (HSP701B)	73,951	5.50	13, 20%	various			
393	65,782	6.06	Arginine methyltransferase (PRMT5/SKB1)	72,786	5.88	27, 38%	5174683	0.7	0.6	0.6
			Vesicle transport-related protein?	70,000	5.75	9, 15%	various			
476	59,114	6.15	Asparaginyl tRNA synthetase (NARS)	62,943	5.90	28, 47%	4758762	0.5	0.2	0.2
680	48,362	5.22	cAMP-dependent protein kinase regulatory subunit 1 (PRKAR1A)	42,982	5.27	17, 37%	4506063	1.5	2.0	2.4
749	44,754	5.06	P47 protein	40,573	4.99	14, 46%	11422183	1.9	2.2	2.4
756	44,304	5.56	HAT1	49,513	5.52	8, 19%	4504341	0.8	0.3	0.5
790	41,658	6.12	Eukaryotic translation initiation factor 3, subunit 4 (eIF3S4)	34,847	6.39	9, 35%	12741583	1.5	1.8	1.9
831	40,712	5.44	Chromosome 14 open reading frame 3 (AHA1)	38,275	5.41	15, 47%	6912280	1.2	1.8	2.0
1025	33,318	4.94	Thioredoxin-like protein 32 kDa (TXNL)	32,252	4.84	11, 37%	4759274	1.1	1.3	1.6
1044	32,738	6.72	HnRNPH3 (2H9)	35,239	6.36	14, 52%	7739440	0.5	0.3	0.3
1091	31,055	6.65	PPRibP synthase (PRPS2)	34,769	6.15	11, 39%	4506129	0.8	0.5	0.4
1100	30,648	5.37	Protein phosphatase 2A catalytic subunit α (PP2A)	35,594	5.3	6, 29%	4506017	0.8	0.5	0.5
1236	25,047	6.03	HSP27-1	22,783	5.98	17, 64%	4504517	1.5	2.1	2.3
1377	16,866	5.12	Similar to HP1δ (CBX3)	20,812	5.22	8, 31%	11421656	1.2	1.6	1.7

NOTE: Cells were treated with a pharmacologically active concentration of 60 nmol/L 17AAG.
Abbreviations: pI, isoelectric point; cAMP, cyclic AMP.
*Calculated from protein markers.
† Calculated from protein database sequence.
‡ Number of matched peptides and their combined sequence coverage for the identified protein; 1 and 2 are proteins identified from matched peptides within a particular spot.

acetylation levels are altered following HSP90 inhibition, suggesting that effects on protein acetylation may potentially play a role in the mechanism of action of HSP90 inhibitors. They also suggest that care should be taken in combining histone deacetylase and HSP90 inhibitors.

The protein arginine methyltransferase PRMT5 is a novel HSP90-binding protein. Consistent with the proteomic analysis data reported earlier (Fig. 2*B*; Table 2), the protein arginine methyltransferase PRMT5 was shown to be depleted by 17AAG in A2780 human ovarian cancer cells over the 72-h time course, with maximum depletion observed at 48 h using immunoblotting (Fig. 4*A, top*). No change in PRMT5 mRNA expression was observed in the cDNA microarray analysis, suggesting that the reduced expression was mediated at the protein level. PRMT5 depletion was shown to be an on-target effect of HSP90 inhibition as it was observed only with growth-inhibitory concentrations of

17AAG and radicicol in A2780 cells and not with the essentially inactive analogue NSC683201 (Fig. 4*A, bottom*). Because depletion following exposure to HSP90 inhibitors is a characteristic of HSP90 client proteins, we hypothesized that this may be the case for PRMT5. Consistent with this hypothesis, immunoprecipitation studies showed that PRMT5 was present in a complex with HSP90, along with the known HSP90 client protein c-RAF-1 (Fig. 4*B*). Identification of PRMT5 in a complex with HSP90 was obtained

Table 3. Functions of annotated proteins

Protein name	Expression trend (increase/ decrease) over time by 17AAG	Gene name	Protein function
Heat shock			
HSP72	Increase	*HSP70-2*	Molecular chaperone
HSC70	Increase	*HSP70-8*	Molecular chaperone
HSP27	Increase	*HSP27*	Molecular chaperone, overexpressed in many estrogen-sensitive human tissues, involved in stabilization/ reorganization of actin cytoskeleton
HSP90α	Decrease/increase/decrease	*HSP90α*	Molecular chaperone
HSP90β	Decrease/increase/decrease	*HSP90β*	Molecular chaperone
HSP70-9B (mortalin-2)	Increase	*HSP70-9B*	Mitochondrial molecular chaperone, causes inactivation of p53 tumor suppressor (35, 57)
AHA1	Increase	*AHA1*	HSP90 cochaperone
Cell cycle/signal transduction			
MCM4	Decrease	*MCM4*	Mini chromosome maintenance protein, involved in chromosome replication, E2F-1 regulated and important for G1/S transition
Protein phosphatase 2A	Decrease	*PP2A*	Important phosphatase in cell cycle regulation and signal transduction. Activity reported to be regulated in some cases by HSF2 (58). Shown to dephosphorylate HSP27
PRMT5	Decrease	*PRMT5*	Methyltransferase, possible link between JAK and PAK signaling, mediator of hyperosmotic stress response
CBX3	Increase	*CBX3* (*HP1*)	HP1 homologue, interacts with nuclear envelope, involved in chromatin assembly
HAT-1	Decrease	*HAT1*	Nucleosome assembly and DNA replication
Metabolic enzymes			
Glucosidase II	Decrease	*G2AN*	Glucose metabolism, important for glycoprotein folding in ER
Glucosamine-fructose-6-phosphate aminotransferase	Decrease	*GFAT* (*GFPT1*)	Catalyzes the formation of glucosamine 6-phosphate in the hexosamine pathway
Asparaginyl tRNA synthetase	Decrease	*NARS*	Aminoacyl-tRNA synthetases are a class of enzymes that charge tRNAs with their cognate amino acids
Phosphoribosyl pyrophosphate synthetase 2	Decrease	*PRPS2*	Involved in purine and pyrimidine metabolism
Transcription/translation			
HnRNP3	Decrease	*HnRNP3*	Involved in early heat shock-induced splicing arrest (59)
Leucine-rich protein	Decrease	*LRPPRC*	Involved in cytoskeletal organisation, vesicular trafficking, transcription and chromosome activity
Eukaryotic translation initiation factor 3, subunit 4	Increase	*EIF3S4*	Translation initiation, evidence of functional link between eIF3 and 26S proteasome
Other			
Annexin 6A	Increase	*ANX6A*	Closely related to a family of proteins that includes intracellular substrates of the EGF receptor and pp60src tyrosine kinases. Thought to bind phospholipids in calcium-dependent manner
Thioredoxin-like protein	Increase	*TXNL1*	Cytoplasmic regulator of redox state
cAMP-dependent protein kinase regulatory subunit	Increase	*PRKAR1A*	Potential tumor suppressor gene, mutated in carney complex tumors
P47	Increase	*P47*	Component of p97 membrane fusion pathway

NOTE: Functions of proteins that had altered expression following 17AAG treatment in A2780 cells. References are provided to recent articles describing these proteins.
Abbreviations: JAK, Janus-activated kinase; PAK, p21-activated kinase; ER, endoplasmic reticulum; EGF, epidermal growth factor; cAMP, cyclic AMP; eIF, eukaryotic translation initiation factor.

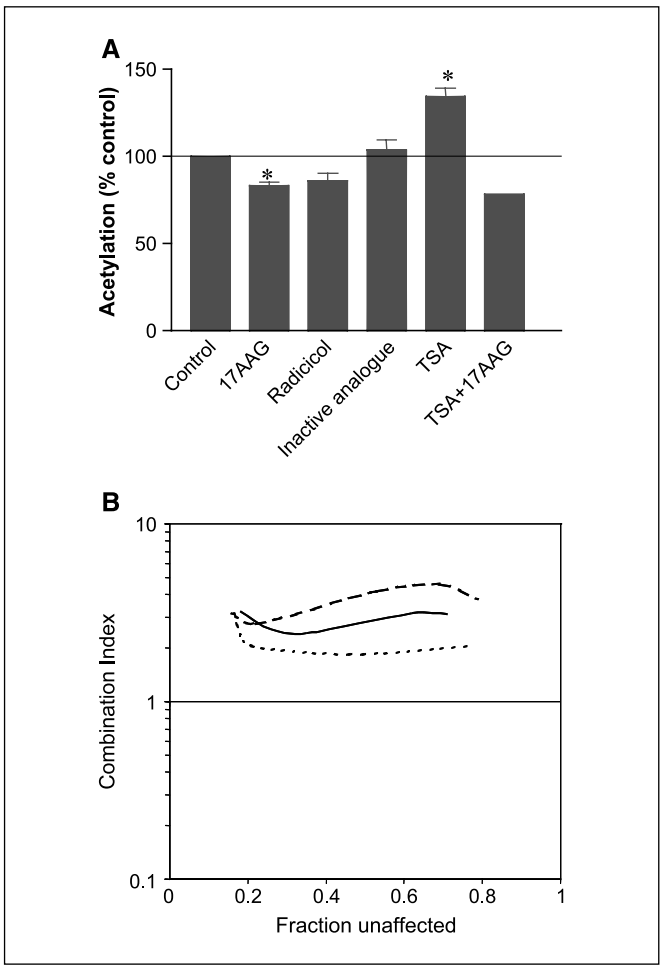

Figure 3. Decreased protein acetylation in A2780 human ovarian cancer cells following HSP90 inhibition. *A,* ELISA to measure acetylation of proteins was carried out on A2780 cells treated with 200 nmol/L 17AAG, radicicol, the essentially inactive 17AAG analogue NSC683201 and TSA. Acetylation was expressed as % control. *Columns,* mean of three independent experiments carried out in duplicate (except TSA + 17AAG; one independent experiment in quadruplicate); *bars,* SD. *B,* median effect analysis of A2780 cells treated with a combination of 17AAG and TSA. Plots of combination index determined using nonexclusive criteria (13) versus fraction of cells unaffected for three independent experiments.

not only by Western blotting (Fig. 4*B*) but also by MS. To check the generality of the depletion of PRMT5 by 17AAG, we also looked at the response of this protein to the drug in the HCT116 human colon cancer and WM266.4 human melanoma cell lines. Figure 4*C* and *D* show that PRMT5 was depleted by 17AAG treatment in both cell lines, as seen above in the A2780 ovarian cancer cells. A time course study of PRMT5 depletion by 17AAG was carried out in WM266.4 melanoma cells, and other relevant biomarkers were also analyzed for direct comparison (Fig. 4*C*). A time-dependent decrease in PRMT5 expression was seen alongside depletion of client proteins c-RAF-1, ERBB2, CDK4, and AKT together with an induction in HSP72 and HSP27. The kinetics of PRMT5 depletion in WM266.4 cells were similar to those seen with the established client protein AKT. In addition to the depletion of PRMT5 by 17AAG and radicicol but not the inactive 17AAG analogue NSC683201, we also carried out experiments with analogues of the novel diaryl pyrazole resorcinol series (5, 27, 28). Consistent with depletion being an on-target effect, PRMT5 expression was decreased by exposure to the more potent inhibitor VER-49009 but not by the much less potent CCT018159 or CCT066961 (data not shown). Thus, PRMT5 is identified as a protein depleted by HSP90 inhibitors and also as a novel binding partner and potential client for HSP90.

Discussion

The aim of this study was to combine both mRNA expression profiling and proteomics to investigate the molecular pharmacology of the HSP90 inhibitor 17AAG. The results illustrate the value of using these two complementary methodologies together to study the molecular responses to cancer drugs. Using this approach, we have identified mRNAs and proteins that are modulated in response to drug treatment and may contribute to the mode of drug action. 17AAG was considered to be a good candidate molecular therapeutic agent to study with this combined approach. This was partly because treatment with the drug is already known to lead to changes in the expression of several mRNAs and proteins, as measured by conventional techniques (29), and partly because there are likely to be complex and incompletely understood molecular effects downstream of HSP90 inhibition. In addition, there is considerable clinical interest in 17AAG that is now in phase II clinical trials (10, 11). We reasoned that a more comprehensive and systematic analysis would be a potentially valuable approach because of its relative lack of bias. This study describes the results of the mRNA and proteomic screening together with follow-up work to validate selected known and new findings and further studies to show the potential significance and therapeutic application of the more novel observations.

The human genome is predicted to encode ~20 to 25,000 proteins (30). Although limitations in two-dimensional gel proteomics technology will restrict detection of certain subsets of proteins (e.g., membrane-bound and low-abundance proteins; ref. 31), ~1,500 proteins from A2780 human ovarian cancer cells were detectable on each two-dimensional gel. Currently, around 100 HSP90 client proteins have been identified.[7] However, it is possible that there are many more proteins that may require HSP90 for their stability and function or which are regulated by HSP90 in other ways. HSP90 client proteins are usually defined as those that bind to HSP90 and are depleted upon treatment of cells with HSP90 inhibitors. Roughly 3% of the proteins identified in the proteomic analysis were shown to be responsive to 17AAG in the A2780 ovarian cancer cell line. Many previously identified HSP90 client proteins were not detected, most likely because of their relatively low abundance in this cell line. For example, c-RAF-1 was not detected. Depletion of this commonly studied client protein was shown using immunoblotting of cell lysates obtained from the same experiment (see Supplementary Fig. S1*A* and *B*), confirming that the 17AAG exposures used in the expression profiling studies were pharmacologically active. Although we expected that c-RAF-1 and other low-abundance clients, particularly signal transduction proteins, would not be detected by the technology used, we reasoned that the approach would potentially be capable of identifying proteins that were not previously known to be responsive to HSP90 inhibitors. We fully recognize that not all proteins responsive to HSP90 inhibitors will be detected. Nevertheless, the usefulness of the approach taken was exemplified

[7] See current list online: http://www.picard.ch/downloads/HSP90interactors.pdf.

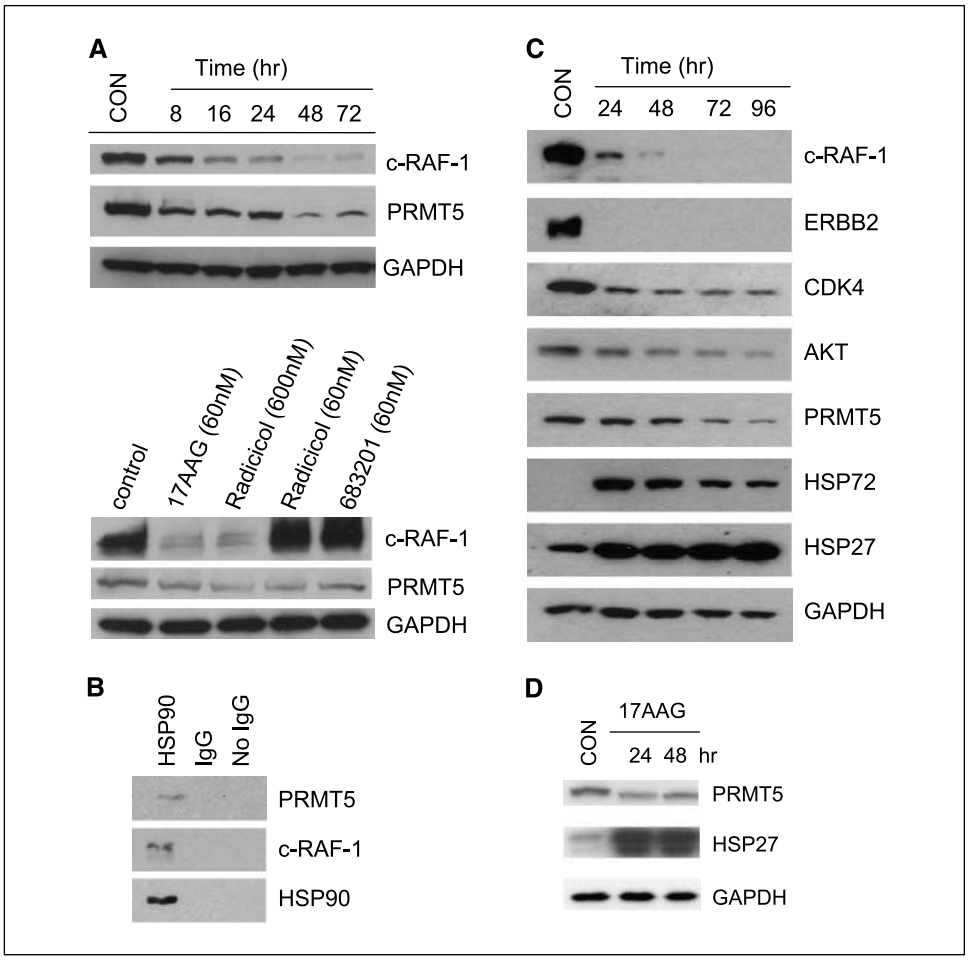

Figure 4. PRMT5 is a novel HSP90 binding partner and potential client protein. *A, top,* protein expression over a 72-h time course following continuous exposure to 60 nmol/L 17AAG in A2780 human ovarian cancer cells. Western blots were done using an antibody against c-RAF-1 and PRMT5. Glyceraldehyde-3-phosphate dehydrogenase (*GAPDH*) was used as a loading control. *Bottom,* altered protein expression following the 24-h exposure to 60 nmol/L 17AAG, 60 and 600 nmol/L radicicol, and 60 nmol/L of the essentially inactive 17AAG analogue NSC683201 in A2780 cells. Western blots were done using antibodies against c-RAF-1 and PRMT5. GAPDH was used as a loading control. *B,* immunoprecipitation was done on A2780 cells using an antibody to HSP90 and an IgG control. An additional control was incubated without the inclusion of any IgG. Western blots of the immunoprecipitated protein were probed with antibodies to c-RAF-1, PRMT5, and HSP90. *C,* altered protein expression changes following the 24- to 96-h continuous exposure of WM266.4 human melanoma cells to 5× IC_{50} 17AAG. Immunoblots were probed with antibodies to c-RAF-1, ERBB2, CDK4, c-AKT, PRMT5, HSP72, HSP27, and GAPDH as loading control. *D,* HCT116 human colon carcinoma cells were exposed to 5× IC_{50} 17AAG for 24 or 48 h. Protein expression was analyzed using antibodies against HSP27 and PRMT5. Glyceraldehyde-3-phosphate dehydrogenase was used as a loading control.

by our identification of several proteins not previously linked with HSP90 inhibition or the cellular response to 17AAG. A number of these need to be investigated further to determine whether they are direct effects of HSP90 inhibition or a result of the downstream consequences of HSP90 blockade. Of particular interest were the changes in chromatin-related proteins and chromatin-modifying enzymes. Given the novelty and potential significance of these findings, we carried out follow-up studies on one of these proteins, the protein arginine methyltransferase PRMT5.

Several 17AAG-responsive proteins were identified that are known to be molecular chaperones. These included HSP90α, HSP90β, HSP72, HSC70, and HSP27, along with the HSP90 ATPase-activating cochaperone AHA1. The induction of HSP90β, HSP72, and HSP27 was shown to be a direct consequence of HSP90 inhibition as defined by their increased expression with both 17AAG and the structurally distinct HSP90 inhibitor radicicol, but not with the essentially inactive 17AAG analogue NSC683201. This analogue was used at a concentration equimolar to that of 17AAG to maximize the likelihood of identifying on-target HSP90 effects as opposed to off-target effects due to the chemical backbone. In addition to the protein changes, the gene expression profiling studies showed that *HSC70* and *HSP90β* expression was induced at the mRNA level following treatment with the active HSP90 inhibitors but not the inactive 17AAG analogue, most likely indicative of the major mechanism of transcriptional regulation of these chaperones involving HSF-1 (32). Interestingly, however, unlike the other molecular chaperones, HSP90α protein expression was also induced by the inactive 17AAG analogue as well as with 17AAG and radicicol, suggesting that this was an off-target effect. Previous reports have indicated that HSP90α is more readily induced by heat shock than by mitogens, whereas the opposite is true for HSP90β, although HSP90β can still be transcriptionally activated by HSF-1 (33, 34). Therefore, HSP90α induction may be indicative of a general stress response, whereas HSP90β is a more robust consequence of HSP90 inhibition.

Induction of both HSP72 and HSC70 isoforms by 17AAG was observed by proteomic analysis in the A2780 ovarian tumor cell line. In addition to these two HSP70 family members, mortalin-2 was shown to be responsive to 17AAG. In addition to its role as a molecular chaperone, mortalin has been shown to regulate p53 activity (35). *HSC70* mRNA expression was also induced, most likely by transcriptional activation by HSF-1. Interestingly, increases in the intensity of multiple protein spots containing HSP90 and HSP70 family members were detected on the two-dimensional gels. This suggests that different posttranslational modifications may be present on these proteins, and further work is required to determine the molecular nature of these forms.

The present study exemplifies in more detail than shown previously the ability of the cell to mobilize an extended repertoire of HSPs as a direct response to HSP90 inhibitors. The up-regulation of a number of these HSP gene products will affect the response of cancer cells to HSP90 inhibitors such as 17AAG. Clearly, increased

expression of HSP90 will replenish the cell reservoir of the drug target and may potentially assist recovery from drug treatment. Cellular recovery may also be aided by up-regulation of the major HSP90 activator AHA1, which as mentioned earlier was initially identified by our combined mRNA and proteomic profiling (23). HSP27, HSP72, HSC70, and HSP90 have been shown to reduce the apoptotic response through a number of different mechanisms (36–38) and could therefore protect the cell against the effects of HSP90 inhibitors. Indeed, a study published while this present study was being finalized has confirmed that HSP27 expression is increased by 17AAG, and that depletion of HSP27 causes sensitization to 17AAG (26).

The expression of an additional chaperone gene *HSP47* was also shown here to be increased by treatment with HSP90 inhibitors. HSP47 is a molecular chaperone that interacts with and stabilizes correctly folded procollagen (39). Procollagen interacts with unfolded polypeptides in the endoplasmic reticulum and increases their period of retention in this organelle, thereby allowing time for adequate protein folding and quality control checks. *HSP47* is transcriptionally regulated by HSF-1 and has been shown to be induced by transforming growth factor-β and interleukins (40). Interestingly, clustering of the gene expression data using a self-organizing map identified a number of mRNAs corresponding to enzymes involved in procollagen function in the same cluster as HSP47 (Fig. 1*B*). A recent study has shown that *HSP47* is silenced by methylation in a number of different tumor types, and that lack of HSP47 results in increased collagen I and IV levels (41). In addition, neuroblastoma cell lines that expressed low levels of HSP47 and high levels of collagen I were highly tumorigenic in nude mice (41). Therefore, HSP47 induction by HSP90 inhibitors could be of therapeutic benefit, at least in some tumor types.

We observed that the heterogeneous nuclear ribonuclear protein hnRNP3 (hnRNP 2H9A) showed decreased expression in response to 17AAG. As a member of the hnRNP H subfamily, this gene shares 78% identity with hnRNP F. Of interest, in addition to the involvement of hnRNP3 in early heat shock–induced splicing arrest (24), a very recent study has reported that several hnRNPs and small heterogeneous nuclear ribonucleoprotein were identified as part of a complex with HSP90, the regulatory and catalytic subunits of DNA-dependent protein kinase, various RNA helicases, poly (ADP-ribose) polymerase-1, and the osmotic regulatory transcription factor (TonEBP/OREBP) in human embryonic kidney cells (42). This suggests a role for the interaction of HSP90 and hnRNPs in regulating gene transcription.

An interesting finding from the cDNA gene expression profiling was the identification of a large number of genes that showed reduced expression in response to HSP90 inhibitors, the levels of which were also decreased in tumor tissue of rectal cancer patients treated with 5-FU (21). This group of genes have been shown by other investigators to be positively regulated by c-MYC (22). *HSP90α* is a target gene of c-MYC, and overexpression and knockout of HSP90 increased or decreased, respectively, the transforming activity of c-MYC in HeLa and RatMyc cells (43). In addition, the HSP90 cochaperone CDC37 has been shown to act as an oncogene and collaborates with cyclin D and c-MYC in cellular transformation (44). It is possible that the decreased expression of the MYC-regulated gene set is a consequence of cell cycle arrest by 17AAG. However, this may also contribute to the therapeutic effects of HSP90 inhibitors.

As mentioned, of particular interest to us was a group of proteins identified in the present proteomic analysis as being responsive to 17AAG and that are known to have a role in chromatin methylation and acetylation. These were HAT-1, the protein arginine methyltransferase PRMT5, and the non-histone protein HP1 protein. Levels of the HP1 protein were increased in response to 17AAG treatment. HP1 interacts with numerous proteins and has been shown to be important in heterochromatin regulation, specifically binding to histone H3 when methylated on Lys^9 by the methyltransferase Suv39 (45). The expression of HAT-1, which is required for DNA replication (46), was decreased following 17AAG treatment. Interestingly, we showed that total protein acetylation was decreased in cells in response to HSP90 inhibitors. There is clearly a complex interaction between protein acetylation and HSP90, not least because it has been reported that histone deacetylase inhibitors may inhibit the chaperone by increasing HSP90 acetylation (47, 48). The link between HSP90 and chromatin biology is also emerging from studies in model organisms (49, 50). The present results suggest further complexity by showing that HSP90 inhibitors reduce the expression of at least one member of each of HAT, protein arginine methyltransferase, and HP families as well as showing that cellular protein acetylation is reduced by 17AAG, even in the presence of an histone deacetylase inhibitor.

The contrasting effects of 17AAG and the histone deacetylase inhibitor TSA on histone acetylation in A2780 ovarian cancer cells suggested the possibility of an antagonistic interaction on cell proliferation. This prediction was confirmed by median effect analysis. In agreement with our findings, another study has shown that geldanamycin inhibits TSA-induced cell death and histone H4 hyperacetylation in COS-7 cells (51). Interestingly, the combination of 17AAG and another histone deacetylase inhibitor SAHA has been shown to be synergistic with respect to apoptosis in leukemia cells (52). This may indicate that the outcome of such combination will be dependent on the type of cancer concerned. Further studies are required to investigate such differences in more detail.

An especially significant finding was our observation of depletion by 17AAG of the protein arginine methyltransferase PRMT5 (53), which led us to identify this chromatin-modifying enzyme as a novel HSP90-binding protein and potential client. Depletion of PRMT5 by 17AAG was reproducibly seen in three different human cancer cell lines (ovarian, colon, and melanoma). PRMT5 showed decreased expression over time following treatment with 17AAG, and the kinetics of depletion was similar to AKT in WM266.4 human melanoma cells. Depletion was shown to be an on-target effect of HSP90 inhibition, as observed by its decreased expression with 17AAG and radicicol but not with the essentially inactive 17AAG analogue NSC683201. In addition, PRMT5 depletion was seen with the potent HSP90-inhibitory diaryl pyrazole resorcinol VER-49009 but not with much less active analogues. Immunoprecipitation studies with analysis by Western blotting and MS confirmed that PRMT5 was complexed with HSP90. This is the first time that a protein arginine methyltransferase has been suggested to be a protein HSP90 client protein. In addition, a recent study has shown that HSP90α enhanced the activity of a lysine-specific histone methyltransferase SMYD3 (54). Modulation of PRMT5 by 17AAG may be of particular significance given that it negatively regulates expression of the *ST7* and *NM23* human suppressor genes (53).

Pharmacodynamic markers are essential for the rational development of molecular therapeutics, including HSP90 inhibitors (10, 55, 56). They can be used to show proof of concept for the proposed mechanism of drug action in phase I studies as well as to help select the optimal dose and schedule. However, the measurement of molecular end points in clinical trials of new

molecular therapeutics remains disappointingly infrequent (25). Simultaneous induction of HSP70 family members accompanied by depletion of client proteins, such as ERBB2, c-RAF-1, and CDK4, was shown to be a characteristic and robust molecular signature of HSP90 inhibition (10, 29, 55). Here, we have extended our molecular profiling studies to show that the expression of HSP27 was not only induced by various HSP90 inhibitors, although not with the less active analogues, but in addition was increased in tumor tissue taken from two patients participating in the phase I clinical trial of 17AAG carried out at our institution (10). Only limited tumor biopsy samples are available from patients treated with 17AAG in the phase I studies. Further studies are required to investigate the significance and broader usefulness of this observation and also the potential value of other potential biomarkers identified in our study. Nevertheless, the result exemplifies how proteomic profiling can identify biomarkers of potential clinical utility. Furthermore, given that HSP27 and HSP70 family members are antiapoptotic (3, 26), the demonstration of the induction of these proteins in human tumor tissue following treatment of patients with 17AAG highlights the importance of considering these molecular responses as potential resistance mechanisms. In addition, the results support the development of inhibitory strategies directed against these antiapoptotic HSPs (26).

In conclusion, the combination of mRNA and protein profiling has confirmed some of the responses already known to occur with 17AAG, thereby validating the methodology. In addition, the combined screening approach has also uncovered a number of very interesting and potentially important proteins and mRNAs not previously known to be affected by 17AAG. The incorporation into this study of an essentially inactive 17AAG analogue and of structurally dissimilar HSP90 inhibitor chemotypes, together with much less active analogues of these, was useful in determining whether molecular changes were likely to be on-target effects of HSP90 inhibition. Protein expression did not always correlate with gene expression changes, illustrating the value of complementary gene profiling and proteomic approaches. Several HSPs and cochaperones were induced in response to HSP90 inhibitors, and, when taken together with depletion of client proteins, these provide a particularly robust molecular signature of HSP90 inhibition. In addition, a number of genes involved in protein synthesis and degradation, RNA processing, transcription, cell cycle, apoptosis, and signal transduction showed altered expression in response to HSP90 inhibitors. The series of mRNA and protein changes observed may shed light on the likely complex mechanism of action of the first-in-class HSP90 inhibitor 17AAG. Of particular novelty and interest were the changes in the expression of proteins involved in chromatin acetylation and methylation. Total cellular acetylation was decreased by treatment with HSP90 inhibitors, providing some evidence that acetylation of histones and other proteins may contribute to the mechanism of action of HSP90 inhibitors. Decreased expression of hnRNP3 suggests possible effects on transcription. These observations add to the accumulating evidence for a dynamic interplay among HSP90, chromatin biology, and gene transcription (49, 50) and suggest that this interaction may have a therapeutic dimension in cancer. Furthermore, based on the demonstration by proteomic profiling of protein depletion by HSP90 inhibition and supported by immunoprecipitation studies, the protein arginine methyltransferase PRMT5 was identified as a protein depleted by HSP90 inhibitors and also as a novel HSP90-binding partner and potential client protein. In addition, the antagonistic effects of 17AAG and TSA on protein acetylation in cells were shown to be associated with an antagonistic interaction on cell proliferation, consistent with the effects of 17AAG on chromatin-modifying enzymes. Another interesting observation was the decreased expression of a group of genes regulated by MYC. These various molecular responses help to shed light on the complex mechanism of action of HSP90 inhibitors and provide potential pharmacodynamic biomarkers of drug effect, including our demonstration of increased HSP27 elevation in tumor tissue of patients receiving 17AAG. Of the various findings emerging from our screen, we regard the novel observations seen with chromatin-modifying enzymes and related proteins as particularly worthy of further study. Finally, because this study has exemplified the value and complementary nature of both gene expression and proteomic profiling in understanding the molecular pharmacology of HSP90 inhibitors, the combined use of these two approaches can be recommended for research on other molecularly targeted therapeutics.

Acknowledgments

Received 8/10/2006; revised 12/28/2006; accepted 1/17/2007.

Grant support: Cancer Research UK [CUK] programme grant C309/A217, Ludwig Institute for Cancer Research, and Institute of Cancer Research studentship (A. Maloney).

The costs of publication of this article were defrayed in part by the payment of page charges. This article must therefore be hereby marked *advertisement* in accordance with 18 U.S.C. Section 1734 solely to indicate this fact.

We thank Dr. Mike Ormerod (The Institute of Cancer Research) for the Combination Index algorithm, Dr. Nick Totty (Cancer Research UK London Research Institute) for help with mass spectrometry of immunoprecipitates, and colleagues in the Workman laboratory for valuable discussion.

References

1. Clarke PA, te Poele R, Workman P. Gene expression microarray technologies in the development of new therapeutic agents. Eur J Cancer 2004;40:2560–91.
2. Petricoin EF, Zoon KC, Kohn EC, Barrett JC, Liotta LA. Clinical proteomics: translating benchside promise into bedside reality. Nat Rev Drug Discov 2002;1:683–95.
3. Calderwood SK, Khaleque MA, Sawyer DB, Ciocca DR. Heat shock proteins in cancer: chaperones of tumorigenesis. Trends Biochem Sci 2006;31:164–72.
4. Whitesell L, Lindquist SL. HSP90 and the chaperoning of cancer. Nat Rev Cancer 2005;5:761–72.
5. Sharp S, Workman P. Inhibitors of the HSP90 molecular chaperone: current status. Adv Cancer Res 2006;95:323–48.
6. Workman P. Combinatorial attack on multistep oncogenesis by inhibiting the Hsp90 molecular chaperone. Cancer Lett 2004;206:149–57.
7. Kelland LR, Sharp SY, Rogers PM, Myers TG, Workman P. DT-Diaphorase expression and tumor cell sensitivity to 17-allylamino, 17-demethoxygeldanamycin, an inhibitor of heat shock protein 90. J Natl Cancer Inst 1999;91:1940–9.
8. Solit DB, Zheng FF, Drobnjak M, et al. 17-Allylamino-17-demethoxygeldanamycin induces the degradation of androgen receptor and HER-2/*neu* and inhibits the growth of prostate cancer xenografts. Clin Cancer Res 2002;8:986–93.
9. Burger AM, Fiebig HH, Stinson SF, Sausville EA. 17-(Allylamino)-17-demethoxygeldanamycin activity in human melanoma models. Anticancer Drugs 2004;15:377–87.
10. Banerji U, O'Donnell A, Scurr M, et al. Phase I pharmacokinetic and pharmacodynamic study of 17-allylamino, 17-demethoxygeldanamycin in patients with advanced malignancies. J Clin Oncol 2005;23:4152–61.
11. Pacey S, Banerji U, Judson I, Workman P. Hsp90 inhibitors in the clinic. Handb Exp Pharmacol 2006;12:331–58.
12. Clarke PA, Hostein I, Banerji U, et al. Gene expression profiling of human colon cancer cells following inhibition of signal transduction by 17-allylamino-17-demethoxygeldanamycin, an inhibitor of the hsp90 molecular chaperone. Oncogene 2000;19:4125–33.
13. Chou TC, Talalay P. Quantitative analysis of dose-effect relationships: the combined effects of multiple drugs or enzyme inhibitors. Adv. Enzyme Regul 1984;22:27–55.

14. Page MJ, Amess B, Townsend RR, et al. Proteomic definition of normal human luminal and myoepithelial breast cells purified from reduction mammoplasties. Proc Natl Acad Sci U S A 1999;96:12589–94.
15. Harris RA, Yang A, Stein RC, et al. Cluster analysis of an extensive human breast cancer cell line protein expression map database. Proteomics 2002;2:212–23.
16. Clauser KR, Hall SC, Smith DM, et al. Rapid mass spectrometric peptide sequencing and mass matching for characterization of human melanoma proteins isolated by two-dimensional PAGE. Proc Natl Acad Sci U S A 1995;92:5072–6.
17. Naaby-Hansen S, Nagano K, Gaffney P, Masters JR, Cramer R. Proteomics in the analysis of prostate cancer. Methods Mol Med 2003;81:277–97.
18. Benvenuti S, Cramer R, Quinn CC, et al. Differential proteome analysis of replicative senescence in rat embryo fibroblasts. Mol. Cell Proteomics 2002;1:280–92.
19. Clark J, Edwards S, John M, et al. Identification of amplified and expressed genes in breast cancer by comparative hybridization onto microarrays of randomly selected cDNA clones. Genes Chromosomes Cancer 2002;34:104–14.
20. Eisen MB, Spellman PT, Brown PO, Botstein D. Cluster analysis and display of genome-wide expression patterns. Proc Natl Acad Sci U S A 1998;95:14863–8.
21. Clarke PA, George ML, Easdale S, et al. Molecular pharmacology of cancer therapy in human colorectal cancer by gene expression profiling. Cancer Res 2003;63:6855–63.
22. Coller HA, Grandori C, Tamayo P, et al. Expression analysis with oligonucleotide microarrays reveals that MYC regulates genes involved in growth, cell cycle, signaling, and adhesion. Proc Natl Acad Sci U S A 2000;97:3260–5.
23. Panaretou B, Siligardi G, Meyer P, et al. Activation of the ATPase activity of hsp90 by the stress-regulated cochaperone aha1. Mol Cell 2002;10:1307–18.
24. Honore B, Vorum H, Baandrup U. hnRNPs H, H′ and F behave differently with respect to posttranslational cleavage and subcellular localization. FEBS Lett 1999;456:274–80.
25. Parulekar WR, Eisenhauer EA. Phase I trial design for solid tumor studies of targeted, non-cytotoxic agents: theory and practice. J Natl Cancer Inst 2004;96:990–7.
26. McCollum AK, Teneyck CJ, Sauer BM, Toft DO, Erlichman C. Up-regulation of heat shock protein 27 induces resistance to 17-allylamino-demethoxygeldanamycin through a glutathione-mediated mechanism. Cancer Res 2006;66:10967–75.
27. Cheung KM, Matthews TP, James K, et al. The identification, synthesis, protein crystal structure and *in vitro* biochemical evaluation of a new 3,4-diarylpyrazole class of Hsp90 inhibitors. Bioorg Med Chem Lett 2005;15:3338–43.
28. Dymock BW, Barril X, Brough PA, et al. Novel, potent small-molecule inhibitors of the molecular chaperone Hsp90 discovered through structure-based design. J Med Chem 2005;48:4212–5.
29. Maloney A, Clarke PA, Workman P. Genes and proteins governing the cellular sensitivity to HSP90 inhibitors: a mechanistic perspective. Curr Cancer Drug Targets 2003;3:331–41.
30. Finishing the euchromatic sequence of the human genome. Nature 2004;431:931–45.
31. Wilkins MR, Gasteiger E, Sanchez JC, Bairoch A, Hochstrasser DF. Two-dimensional gel electrophoresis for proteome projects: the effects of protein hydrophobicity and copy number. Electrophoresis 1998;19:1501–5.
32. Zou J, Guo Y, Guettouche T, Smith DF, Voellmy R. Repression of heat shock transcription factor HSF1 activation by HSP90 (HSP90 complex) that forms a stress-sensitive complex with HSF1. Cell 1998;94:471–80.
33. Stephanou A, Latchman DS. Transcriptional regulation of the heat shock protein genes by STAT family transcription factors. Gene Expr 1999;7:311–9.
34. Han SI, Oh SY, Woo SH, et al. Implication of a small GTPase Rac1 in the activation of c-Jun N-terminal kinase and heat shock factor in response to heat shock. J Biol Chem 2001;276:1889–95.
35. Wadhwa R, Taira K, Kaul SC. An Hsp70 family chaperone, mortalin/mthsp70/PBP74/Grp75: what, when, and where? Cell Stress Chaperones 2002;7:309–16.
36. Mehlen P, Schulze-Osthoff K, Arrigo AP. Small stress proteins as novel regulators of apoptosis. Heat shock protein 27 blocks Fas/APO-1- and staurosporine-induced cell death. J Biol Chem 1996;271:16510–4.
37. Beere HM, Wolf BB, Cain K, et al. Heat-shock protein 70 inhibits apoptosis by preventing recruitment of procaspase-9 to the Apaf-1 apoptosome. Nat Cell Biol 2000;2:469–75.
38. Pandey P, Saleh A, Nakazawa A, et al. Negative regulation of cytochrome *c*-mediated oligomerization of Apaf-1 and activation of procaspase-9 by heat shock protein 90. EMBO J 2000;19:4310–22.
39. Tasab M, Batten MR, Bulleid NJ. Hsp47: a molecular chaperone that interacts with and stabilizes correctly-folded procollagen. EMBO J 2000;19:2204–11.
40. Sasaki H, Sato T, Yamauchi N, et al. Induction of heat shock protein 47 synthesis by TGF-beta and IL-1 beta via enhancement of the heat shock element binding activity of heat shock transcription factor 1. J Immunol 2002;168:5178–83.
41. Yang Q, Liu S, Tian Y, et al. Methylation-associated silencing of the heat shock protein 47 gene in human neuroblastoma. Cancer Res 2004;64:4531–8.
42. Chen Y, Schnetz MP, Irarrazabal CE, et al. Proteomic identification of proteins associated with the osmoregulatory transcription factor TonEBP/OREBP; functional effects of Hsp90 and PARP-1. Am J Physiol Renal Physiol 2006. Epub ahead of print 2006 Dec 5.
43. Teng SC, Chen YY, Su YN, et al. Direct activation of HSP90A transcription by c-Myc contributes to c-Myc-induced transformation. J Biol Chem 2004;279:14649–55.
44. Stepanova L, Finegold M, DeMayo F, Schmidt EV, Harper JW. The oncoprotein kinase chaperone CDC37 functions as an oncogene in mice and collaborates with both c-*myc* and cyclin D1 in transformation of multiple tissues. Mol Cell Biol 2000;20:4462–73.
45. Kamakaka RT. Heterochromatin: proteins in flux lead to stable repression. Curr Biol 2003;13:R317–9.
46. Verreault A, Kaufman PD, Kobayashi R, Stillman B. Nucleosomal DNA regulates the core-histone-binding subunit of the human Hat1 acetyltransferase. Curr Biol 1998;8:96–108.
47. Yu X, Guo ZS, Marcu MG, et al. Modulation of p53, ErbB1, ErbB2, and Raf-1 expression in lung cancer cells by depsipeptide FR901228. J Natl Cancer Inst 2002;94:504–13.
48. Bali P, Pranpat M, Bradner J, et al. Inhibition of histone deacetylase 6 acetylates and disrupts the chaperone function of heat shock protein 90: a novel basis for antileukemia activity of histone deacetylase inhibitors. J Biol Chem 2005;280:26729–34.
49. Sangster TA, Queitsch C, Lindquist S. Hsp90 and chromatin: where is the link? Cell Cycle 2003;2:166–8.
50. Zhao R, Davey M, Hsu YC, et al. Navigating the chaperone network: an integrative map of physical and genetic interactions mediated by the hsp90 chaperone. Cell 2005;120:715–27.
51. Huang HC, Liu YC, Liu SH, Tzang BS, Lee WC. Geldanamycin inhibits trichostatin A-induced cell death and histone H4 hyperacetylation in COS-7 cells. Life Sci 2002;70:1763–75.
52. Rahmani M, Yu C, Dai Y, et al. Coadministration of the heat shock protein 90 antagonist 17-allylamino- 17-demethoxygeldanamycin with suberoylanilide hydroxamic acid or sodium butyrate synergistically induces apoptosis in human leukemia cells. Cancer Res 2003;63:8420–7.
53. Pal S, Vishwanath SN, Erdjument-Bromage H, Tempst P, Sif S. Human SWI/SNF-associated PRMT5 methylates histone H3 arginine 8 and negatively regulates expression of ST7 and NM23 tumor suppressor genes. Mol Cell Biol 2004;24:9630–45.
54. Hamamoto R, Furukawa Y, Morita M, et al. SMYD3 encodes a histone methyltransferase involved in the proliferation of cancer cells. Nat Cell Biol 2004;6:731–40.
55. Banerji U, Walton M, Raynaud F, et al. Pharmacokinetic-pharmacodynamic relationships for the heat shock protein 90 molecular chaperone inhibitor 17-allylamino, 17-demethoxygeldanamycin in human ovarian cancer xenograft models. Clin Cancer Res 2005;11:7023–32.
56. Zhang H, Chung D, Yang YC, et al. Identification of new biomarkers for clinical trials of Hsp90 inhibitors. Mol Cancer Ther 2006;5:1256–64.
57. Kaul SC, Yaguchi T, Taira K, Reddel RR, Wadhwa R. Overexpressed mortalin (mot-2)/mthsp70/GRP75 and hTERT cooperate to extend the *in vitro* lifespan of human fibroblasts. Exp Cell Res 2003;286:96–101.
58. Hong Y, Sarge KD. Regulation of protein phosphatase 2A activity by heat shock transcription factor 2. J Biol Chem 1999;274:12967–70.
59. Mahe D, Mahl P, Gattoni R, et al. Cloning of human 2H9 heterogeneous nuclear ribonucleoproteins. Relation with splicing and early heat shock-induced splicing arrest. J Biol Chem 1997;272:1827–36.

Gene and Protein Expression Profiling of Human Ovarian Cancer Cells Treated with the Heat Shock Protein 90 Inhibitor 17-Allylamino-17-Demethoxygeldanamycin

Alison Maloney, Paul A. Clarke, Soren Naaby-Hansen, et al.

Cancer Res 2007;67:3239-3253.